

Original Article

Robust Human Activity Recognition using Equilibrium Optimizer with Deep Extreme Learning Machine Model

L. Maria Anthony Kumar¹, S. Murugan², A. Therasa Alphonsa³

¹Department of Computer and Information Science, Annamalai University, Annamalai Nagar, Tamil Nadu, India.

²Dr. M.G.R. Government Arts and Science College for Women, Villupuram.

³Department of Chemistry, Government Arts College, C-Mutlur, Chidambaram.

¹Corresponding Author : lmakumarphd@gmail.com

Received: 26 February 2023

Revised: 06 April 2023

Accepted: 01 May 2023

Published: 29 May 2023

Abstract - Recently, Human Activity Recognition (HAR) is becoming one of the prevalent study fields. HAR is a powerful tool for monitoring a person's dynamism, and it can be accomplished through machine learning (ML) techniques. HAR is a technique of automatically analysing and recognizing human activities depending on information from several wearable devices and smartphone sensors, like location, accelerometer, gyroscope, duration, and other environmental sensors. This study introduces a new Robust Human Activity Recognition using Equilibrium Optimizer with Deep Extreme Learning Machine (RHAR-EODELM) model. The presented RHAR-EODELM technique mainly identifies different classes of human activities. It follows a three-stage process. Initially, the RHAR-EODELM technique employs a min-max normalization process for scaling the activity data. Next, the RHAR-EODELM technique exploits a deep extreme learning machine with a radial basis function (DELm-RBF) model for the prediction process. Finally, the EO approach is enforced to adjust the parameters associated with the DELm-RBF method. A large-scale simulating process highlights the improved HAR results of the RHAR-EODELM method. The experimental values signify that the RHAR-EODELM method reaches improved predictive outcomes over other models.

Keywords - Activity recognition, Brain-computer interface, Equilibrium optimizer, Machine learning, Parameter tuning.

1. Introduction

Recently, the research community has focused much on the domain of Human Activity Recognition (HAR), so the large scale of its real-world applications in real-time usages, like surveillance by authorities, biometric user detection, and health monitoring of elderly persons [1]. Several types of research on HAR are increasing rapidly as sensors are more broadly accessible, power and cost consumption have diminished due to technological advancements in machine learning techniques. The Internet of Things (IoT) and Artificial Intelligence (AI) can be streamed live [2]. The development of HAR has enabled real-time applications in many real-time areas that comprises the healthcare field, the recognition of violence and crime, tactical military applications and sports science [3]. Mathematical methods, depending on HAR info, consent to the detection of various human actions, for instance, standing, running, walking, and sitting [4].

Many difficulties in HAR occur; for instance, biometric user detection can use HAR detection techniques to capture the person behavioural paradigms of an individual [5, 6], like motion capture signs, as biometric is a science in which

efficiency for detecting person, related to their features for accessing devices without authorization, was learned [7]. Currently, the basis of biometric detection mainly includes the physiological property of an individual. However, strong concerns concerning HAR and privacy are imposed by such physiological features [8], which are observed as a feasible substitute, working just as a system for behavioural biometrics. Currently, both technology to process sensor data and sensor technology have progressed [9]. The outstanding presentation of deep learning (DL) in speech recognition and image recognition has promoted the implementation of DL in sensor-related HAR [10, 11, 12] and authors have proven that better performance can be achieved through DL. The three-axis accelerometer was typically utilized sensor in sensor-related HAR [13, 14]. So, integrating the features of HAR technology and embedded technology for studying the application of HAR systems related to convolutional neural networks (CNN) on embedded platforms includes some practical values for developing AI marginalization [15, 16].

This study introduces a new Robust Human Activity Recognition using Equilibrium Optimizer with a deep



extreme learning machine (RHAR-EODELM) model. The presented RHAR-EODELM technique mainly identifies different classes of human activities. It follows a three-stage process. Initially, the RHAR-EODELM technique employs a min-max normalization process for scaling the activity data. Next, the RHAR-EODELM technique exploits a deep extreme learning machine with a radial basis function (DELM-RBF) model for the prediction process. Finally, the EO approach is enforced to adjust the parameters associated with the DELM-RBF method. A large-scale simulating process is performed to highlight the improved HAR results of the RHAR-EODELM method.

2. Related Works

Santosh Kumar Yadav et al. [17] present a technique called novel deep convolutional LSTM (ConvLSTM) networking for skeleton-related activity detection and fall recognition. ConvLSTM networking was a serial hybrid of fully connected layers, CNNs, and LSTM networks. The acquisition mechanism implements pose estimation and human detection for pre-calculating skeletal coordinates from imageries or video series. To build the new guided features, the ConvLSTM method utilizes the basic skeleton coordinates in addition to their characteristic kinematic and geometrical attributes. Muhammad Bilal et al. [18] devised a DL-oriented spatial and temporal HAR structure for overlapping human activities in long videos. TL methods were utilized for extracting the in-depth features. Optimally pre-trained CNN-tuned methods study spatial relations at the framing stage. An optimum Deep AE has been utilized to squeeze high-dimension in-depth features. An LSTM with RNN has been utilized for learning the long-term temporal relation.

Young Li and Luping Wang [19] present a DL method related to bi-directional LSTM (BiLSTM) and residual block. The method initially extracted spatial factors of multi-dimensional signalling of MEMS inertial nodes mechanically utilizing residual blocking and gains the backward and forward dependency of factor serial utilizing Bi-LSTM. At last, the attained features were given into the Softmax layer for completing the HAR. Imran Ullah Khan et al. [20] suggested a fusion method incorporating LSTM and CNN for recognizing activity. In contrast, CNN was implemented for the spatial extracting of features, and the LSTM network can be used for temporal information learning.

Huaijun Wang et al. [21] present a DL-related technique that can identify particular actions and transitions among two discrete actions of less frequency and a short period for healthcare applications. In this article, the authors construct a deep CNN to derive attributes from sensor data. Afterwards, the LTSM network was utilized to capture long-term dependency between two activities to enhance the HAR

recognition rate. By integrating LSTM and CNN, a wearable sensor-oriented technique was devised to recognize actions and their transitions precisely. Ohoud Nafea et al. [22] introduced a new technique utilizing CNN with changing kernel dimensions and bi-directional LSTM (BiLSTM) for capturing attributes at different resolutions. The originality of the present study falls in the potential choice of optimum video depictions and the potential extracting of spatiotemporal factors from sensor info utilizing Bi-LSTM and conventional CNN. The authors [23] offered a supervised dual-channel method that contains an attention system and LSTM. The authors even introduced an adaptive channel-squeezing operation for fine-tuning CNN feature extraction ability through multichannel dependency.

3. The Proposed Model

In this research, an automated activity recognition method called the RHAR-EODELM model is developed. The presented RHAR-EODELM technique mainly identified different classes of human activities. It follows a three-phase procedure: preprocessing, activity recognition using DELM-RBF, and an EO-based tuning process. Figure 1 represents the workflow of the RHAR-EODELM model.

3.1. Data Preprocessing

Firstly, the RHAR-EODELM technique employs a min-max normalizing procedure to scale the activity info. The standard scalar method can eliminate the mean and scaling info into the unit discrepancy. The main idea behind the standard scalar technique is that it converted the information to dispersion, holding an average value of 0 and a standard deviating value of 1. For multi-variable data, the preprocessing was carried out factor-wise. For a presented data dispersion, all distinct values in the dataset have deducted mean values and then categorized by the standard deviation of the complete dataset.

3.2. Activity Recognition using DELM-RBF Model

The RHAR-EODELM approach exploited the DELM-RBF model for the prediction approach in this research. Huang et al. developed an ELM feedforward network with one hidden layer (HL) and three modules: hidden, input, and output neurons [24]. Figure 2 demonstrates the framework of ELM. The DELM has lately attracted the interest of several research workers. It overcomes various problems in a way that other approaches cannot owe to assurance of a particular level of learning accuracy, more vital generalization ability, and lower reliance on manual intervention. It saves a cost and a great deal of time than CNN. There exist N unique instances (x_i, y_i) for the classification problems, where $x_i = [x_{i1}, x_{i2}, \dots, x_{in}]^T \in R^n$ represents the sample input vector and $y_i = [y_{i1}, y_{i2}, \dots, y_{im}]^T \in R^m$ denotes the output vector, whereas n shows the feature numbers of training samples, and m indicates the overall amount of training samples.

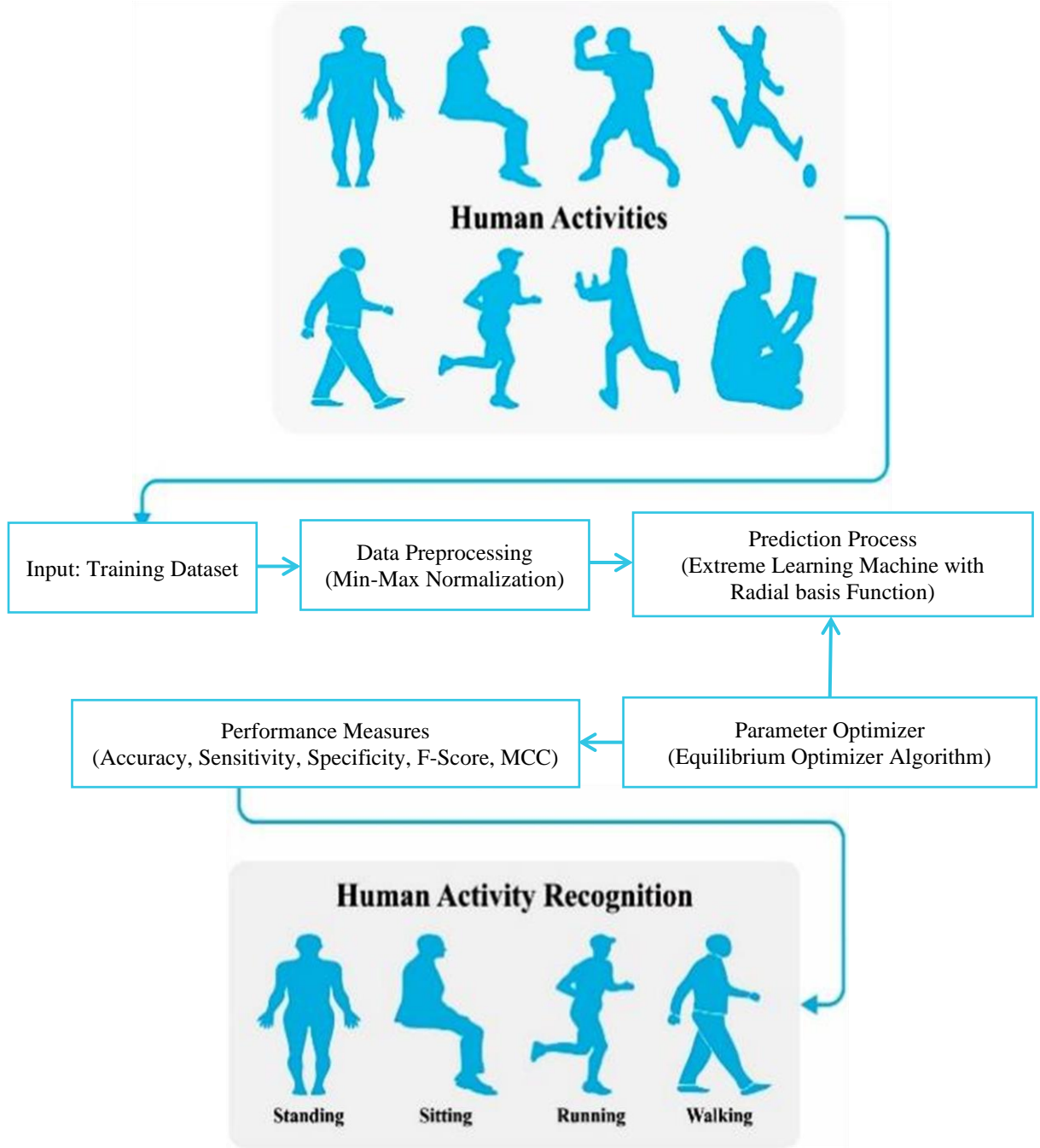


Fig. 1 Workflow of RHAR-EODELM algorithm

L specifies the nodes utilized in the HL of ELM. The output of ELM is expressed as follows:

$$\sum_{i=1}^L \Omega_i g(\omega_i \cdot x_j + u_i) = Q_j, j = 1, 2, \dots, N \quad (1)$$

In Eq. (1), $g(\bullet)$ indicates the activation function, and $\omega_i = [\omega_{i1}, \omega_{i2}, \dots, \omega_{in}]^T$ represent the inputted weightage

vector that interconnects the nodes of the inputted layer to the HL node. $\Omega_i = [\Omega_{i1}, \Omega_{i2}, \dots, \Omega_{in}]^T$ specifies the resulting weightage vector that will act as a linkage connecting the output layer and the HL sensors. u_i denotes the offset value of the initial sensor in the HL. $\omega_i \cdot x_j$ shows the weight allocated to the innermost product and the training sample values.

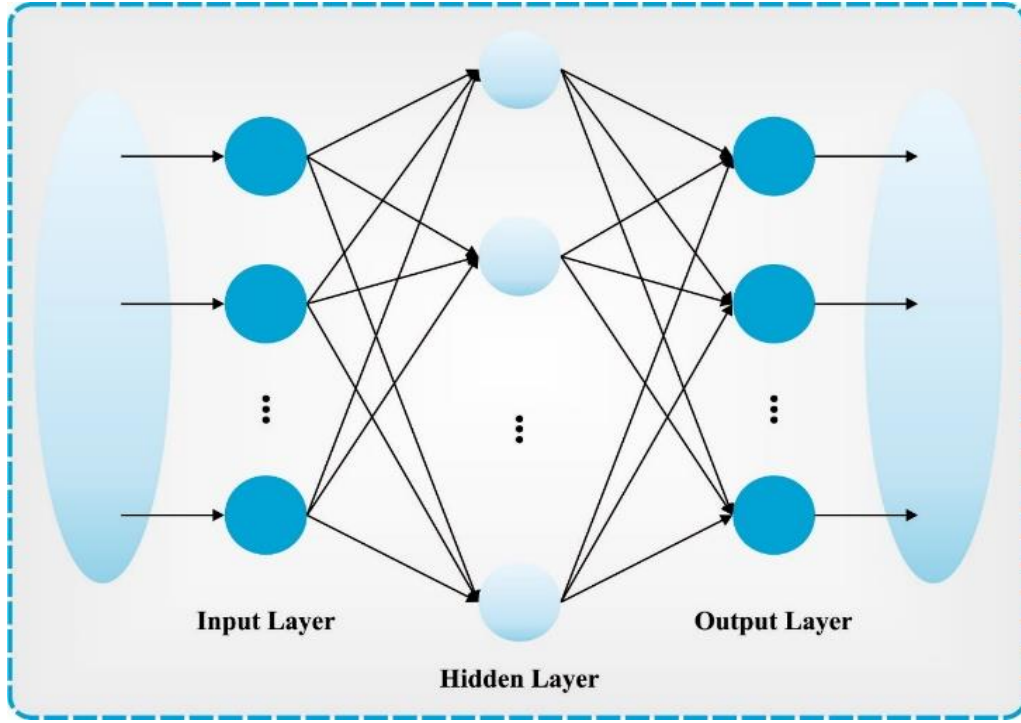


Fig. 2 ELM structure

Q_j indicates the actual output of the network. The presented method aims to minimize the error value of the output using the following equation:

$$\sum_{j=1}^N \| Q_j - y_j \| = 0 \quad (2)$$

In Eq. (2), y_j denotes predicted output, and $\| \cdot \|$ represents the bounded operators between normal spaces:

$$\sum_{i=1}^L \Omega_i g(\omega_i \cdot x_i + u_i) = y_j, j = 1, 2, \dots, N \quad (3)$$

The subsequent simplification of Eq. (3) can be made Based on the matrix:

$$H\Omega = T \quad (4)$$

In Eq. (4), H represents the resulting value matrix of HL, Ω shows the reweighting matrices extending from the HL to the resulting layer, and T signifies the predictable resulting matrices. Furthermore, T and Ω are formulated as:

$$H = \begin{bmatrix} g(\omega_1 \cdot x_1 + u_1) & g(\omega_L \cdot x_1 + u_L) \\ \vdots & \vdots \\ g(\omega_1 \cdot x_N + u_1) & g(\omega_L \cdot x_N + u_L) \end{bmatrix}_{N \times L} \quad (5)$$

$$\Omega = \begin{bmatrix} \Omega_1^T \\ \vdots \\ \Omega_L^T \end{bmatrix}_{L \times m} \quad (6)$$

$$T = \begin{bmatrix} y_1^T \\ \vdots \\ y_L^T \end{bmatrix} \quad (7)$$

The formula $H\Omega = T$ could not be illustrated in most cases. Many conditions are defined for training the network, along with Ω_i , ω_i , and u_i . The following formula illustrates the importance of altering these conditions to accomplish the least potential error:

$$\| H(\omega_i, u_i)\Omega_i - T \| = \min_{\omega_i, \Omega_i, u_i} \| H(\omega_i, u_i)\Omega_i - T \| \quad (8)$$

Algorithm 1: Typical DELM Process
Input: Activation function $g(\bullet)$ #Neurons of HL L N training instances (x_i, y_i) , $x_i \in R^n, y_i \in R^m, i \in \{1, 2, \dots, N\}$.
Output: The resulting weight Ω from the HL to the output layer.
Begin Randomly initialize the input weight ω_i and the offset of HL u_i Compute the output weight of HL H Compute the resulting weight from HL to the resulting layer Ω . End

ELM is strongly recommended because it includes simple implementation that needs lesser time spent on training, without iteration adjustment, and has excellent generalizability.

Unlike DELM, DELM-RBF implements RBF kernel rather than the SLFN for improving model performance [25]. The cluster centres and influence widths of the RBF kernel can be initialized arbitrarily. Besides, the resultant of HLs is connected to the particular tasking.

For sample, in multiple label classifier, dimensional outcome was equivalent to the count of classes. Besides, the kernel function in DELM-RBF has been formulated as Eq. (9).

$$h_k(x) = h(c_k, \sigma_k, x) = \exp(-\|x - c_k\|^2 / (\sigma_k^2)), k = 1, 2, \dots, K \quad (9)$$

whereas χ refers to the inputted vector. c_k signifies the centre of the k^{th} cluster from the RBF kernel, and σ_k implies the influence width of the clustering. The outcome of DELM-RBF is exposed in Eq. (10).

$$f(x) = \sum_{i=1}^L \beta_i h_j(x) = h(x)\beta \quad (10)$$

whereas β_i represents the resultant weight. The optimized target of DELM-RBF was defined as:

$$H\beta = T \quad (11)$$

In which H demonstrates the resultant matrix of HL, and T refers to the outcome labelling matrix. It represents that RBF function is vital in the novel ELM system and its improved methods. RBF function is a significant standard activating function of ELM, and it was also the critical K-ELM's kernel style. It can be reasonable to consider that an improved ELM technique utilizing RBF function as an important infrastructure like DELM-RBF will be an effectual system.

3.3. Parameter Tuning using EO Algorithm

In the last phase, the EO approach is implemented for parameter altering associated with the DELM-RBF approach. EO is a metaheuristic algorithm that relies on the law of physics and is used to balance mass in equilibrium and dynamic states [26, 27]. This technique could resolve multi-engineering issues such as PV parameter estimation, image recognition and power systems. The study exploits EO for tracking the GMPP under partial shade settings. To implement the EO technique, the 3 phases need to be followed.

3.3.1. Initialization

This phase gathers the group of particles where all the particles have a resolution for optimizing the problem. During the random searching, primary vector concentration is produced using the following expression:

$$X_i^{\text{initial}1} = X_{lb} + (X_{ub} - X_{lb}) \times \text{rand}_i, i = 0, 1, 2, \dots, np \quad (12)$$

In Eq. (12), $X_i^{\text{initial}1}$ specifies the particle concentration vector, ub and lb indicate the upper and upper limits for the dimension, np indicates the number of particles, and the rand is the randomly generated w_i^{th} particle ranges from zero to one.

3.3.2. Equilibrium Pool and Candidates

The EO search for a state of equilibrium; If it reaches the near-optimum resolution for the optimizing problems, it can be named an equilibrium state. Generally, the EO does not standardize the concentration level under the optimization technique. Consequently, EO assigns the four most productive particles and the arithmetical mean to improve exploitation and exploration as demonstrated in Eq. (13). From these Equations; the equilibrium pooling is attained and used to generate a vector.

$$\vec{D}_{\text{eq.pool}} = \{\vec{D}_{\text{eq.(1)}}, \vec{D}_{\text{eq.(2)}}, \dots, \vec{D}_{\text{eq.(n)}}, \vec{D}_{\text{eq.(avg)}}\} \quad (13)$$

Here, all the particles are upgraded in concentration for each iteration.

3.3.3. Concentration Update

The term exponential (F) is utilized to upgrade the concentrating process, as demonstrated in Eq. (14). This is highly effective in upgrading the investigation and exploiting method.

$$\vec{F} = e^{-\vec{\lambda}(t-t_0)} \quad (14)$$

In Eq. (14), λ indicates a random vector within [0, 1], and t signifies the iterating time. The t value is minimized with maximum iterating. The selection of fitness was a crucial feature of the EO method. Solution encoding is employed to measure the goodness of the candidature resolution. The precision values are the major state employed in designing a fitness function.

$$\text{Fitness} = \max(P) \quad (15)$$

$$P = \frac{TP}{TP+FP} \quad (16)$$

From the above expression, TP and FP signify the true and false positive values.

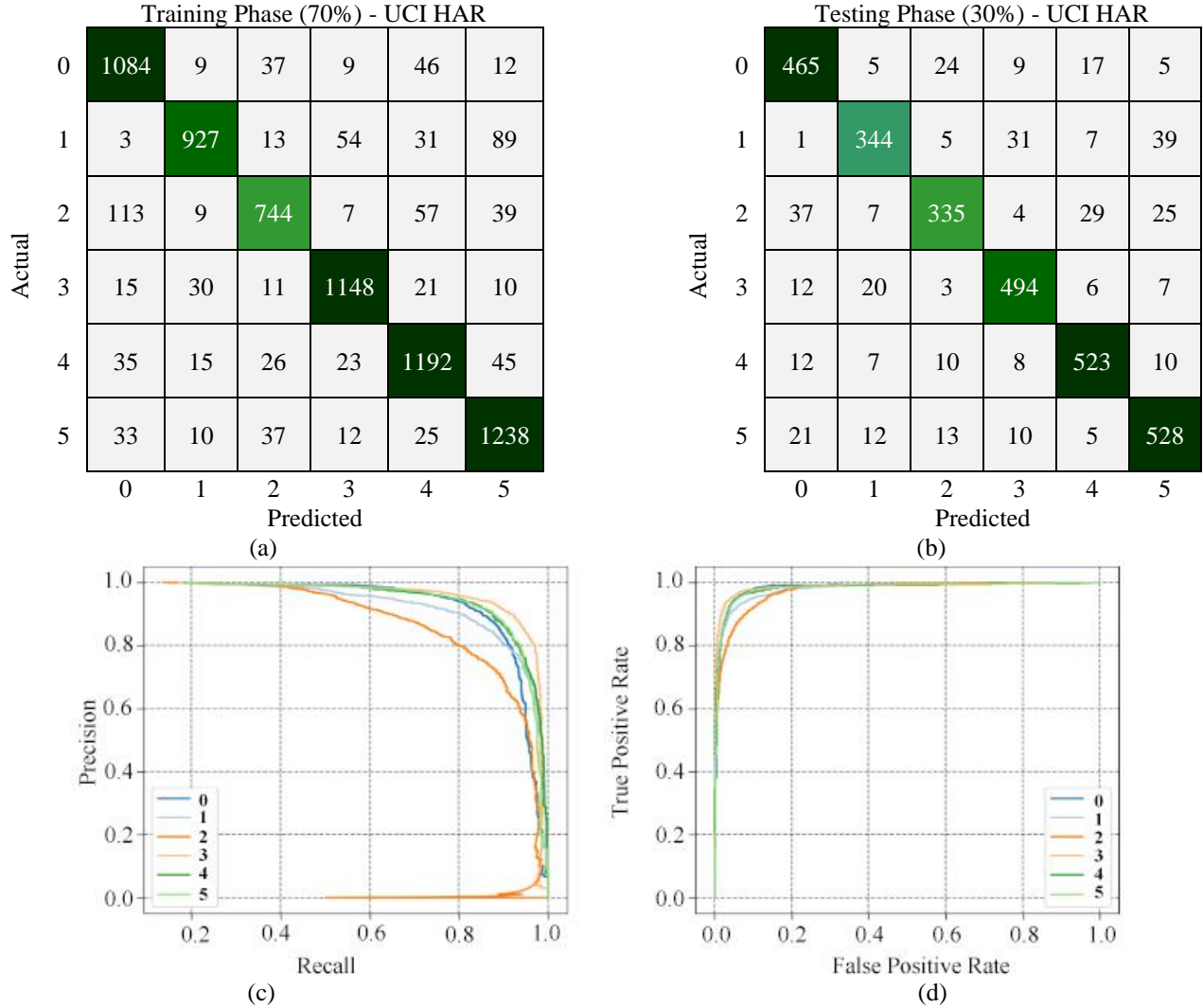


Fig. 3 Classifier outcome of UCI HAR dataset (a-b) 70:30 of TRS/TSS, (c) PR, and (d) ROC

4. Results and Discussion

In the given segment, the experimental validation of the RHAR-EODELM approach can be examined by implementing two datasets [28, 29]. Table 1 and Table 2 represent the details of two datasets. Figure 3 shows the classifier outputs of the RHAR-EODELM approach under the UCI HAR dataset. Figure 3a shows the confusion matrix extracted by the RHAR-EODELM method on 70% of TRS. The figure demonstrated that the RHAR-EODELM methodology had recognized 1084, 927, 744, 1148, 1192, and 1238 instances under classes 0-5. Also, Figure 3b portrays the confusion matrices presented by the RHAR-EODELM approach on 30% of TSS. The figure represented that the RHAR-EODELM approach has recognized 465, 344, 335, 494, 523, and 528 instances under classes 0-5. Similarly, Figure 3c shows the PR investigation of the RHAR-EODELM technique. The figures described that the RHAR-EODELM model had gained extreme PR

accomplishment under the total classes. Lastly, Figure 3d represent the RHAR-EODELM model's ROC study. The figure exhibited that the RHAR-EODELM model has capable outcomes with maximum ROC values in discrete class labelling.

Table 3 and Figure 4 show HAR outcomes of the RHAR-EODELM technique with 70:30 TRS/TSS under the UCI HAR dataset. The experimental outputs represent that the RHAR-EODELM approach has recognized distinct classes. As a sample, with 70% of TRS, the RHAR-EODELM approach attains an average acc_y of 95.95%, $sens_y$ of 87.31%, $spec_y$ of 97.56%, F_{score} of 87.52%, and MCC of 85.17%. Also, with 30% of TSS, the RHAR-EODELM approach attains average acc_y of 95.67%, $sens_y$ of 86.39%, $spec_y$ of 97.39%, F_{score} of 86.59%, and MCC of 84.16%.

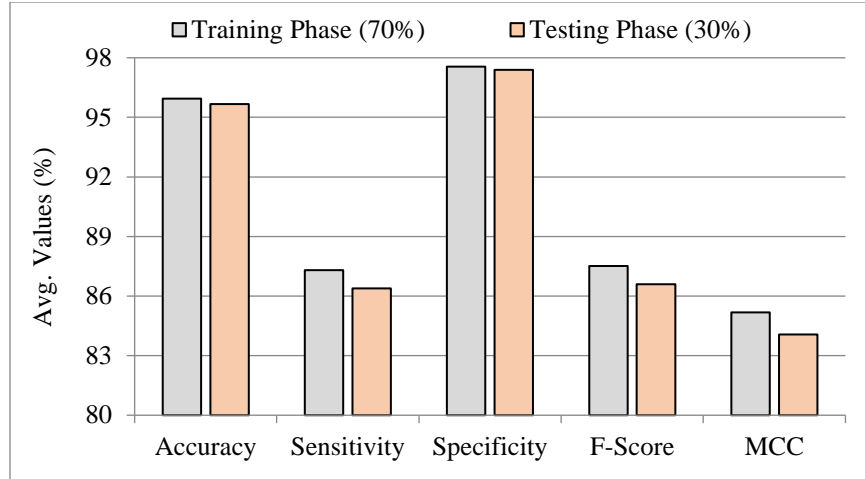


Fig. 4 Average result of RHAR-EODELM technique on UCI HAR database

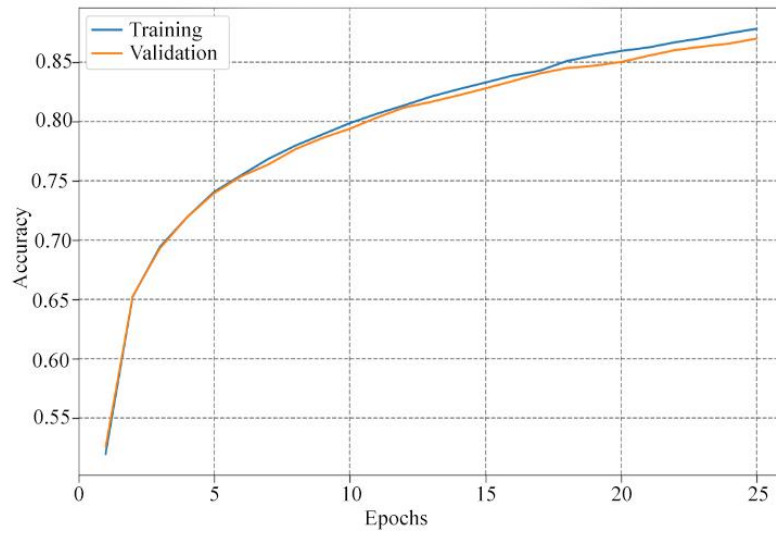


Fig. 5 TACC and VACC outcome of RHAR-EODELM technique on UCI HAR database

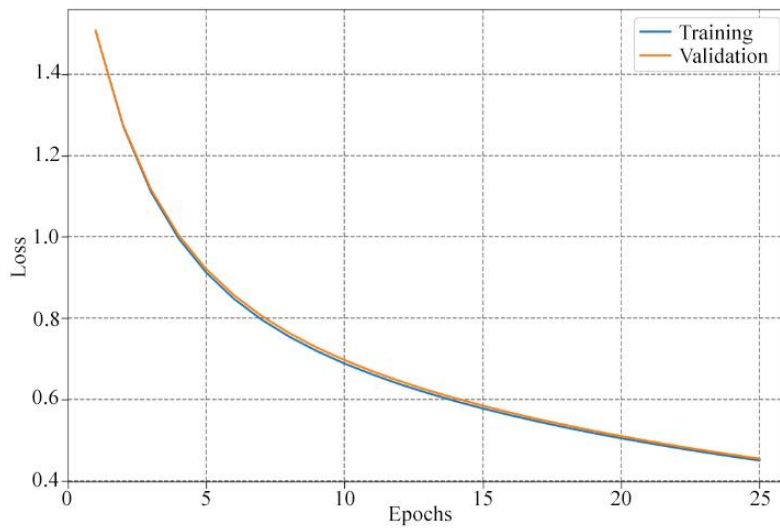


Fig. 6 TLOS and VLOS outcome of RHAR-EODELM technique on UCI HAR database

Table 1. UCI HAR dataset details

UCI HAR		
Label	Class	Instance Numbers
0	Walking	1722
1	Walk-Toward-Upstairs	1544
2	Walk-Toward-Downstairs	1406
3	Sit-Position	1777
4	Stand-Position	1906
5	Lying	1944
Total Instances		10299

Table 2. Details of the USC HAD dataset

USC HAD		
Label	Class	No. of Instances
0	Walking-Left	70
1	Walk-Toward-Downstairs	70
2	Running-Forward	70
3	Stand-Position	70
4	Sleep-Position	70
5	Elevating-Up	70
Total No. of Instances		420

Table 3. HAR outcome of RHAR-EODELM technique with 70:30 of TRS/TSS on UCI HAR dataset

UCI HAR					
Class	$Accu_y$	$Sens_y$	$Spec_y$	F_{score}	MCC
Training Phase (70%)					
0	95.67	90.56	96.69	87.42	84.88
1	96.35	82.99	98.80	87.58	85.63
2	95.16	76.78	98.01	81.00	78.39
3	97.34	92.96	98.24	92.28	90.68
4	95.51	89.22	96.94	88.04	85.28
5	95.67	91.37	96.67	88.81	86.18
Average	95.95	87.31	97.56	87.52	85.17
Testing Phase (30%)					
0	95.37	88.57	96.76	86.67	83.90
1	95.66	80.56	98.08	83.70	81.28
2	94.92	76.66	97.93	81.02	78.26
3	96.44	91.14	97.57	89.98	87.83
4	96.41	91.75	97.46	90.41	88.21
5	95.24	89.64	96.56	87.78	84.86
Average	95.67	86.39	97.39	86.59	84.06

The TACC and VACC values of the RHAR-EODELM algorithm on the UCI HAR data are represented in Figure 5. The figure presented that the RHAR-EODELM model has depicted an enhanced accomplishment with an enhanced TACC and VACC values. In particular, the RHAR-EODELM algorithm has maximal TACC outputs.

The TLOS and VLOS of the RHAR-EODELM algorithm on the UCI HAR data are represented in Figure 6. The figure exhibited that the RHAR-EODELM model has advanced achievement with minimal TLOS and VLOS values. The RHAR-EODELM algorithm has decreased VLS outputs.

Figure 7 depicts the classifier outcomes of the RHAR-EODELM method under the USC HAD dataset. Figure 7a exhibits the confusion matrix presented by the RHAR-EODELM method on 70% of TRS. The figure represented that the RHAR-EODELM approach has recognized 45, 42, 42, 45, 41, and 43 instances under classes 0-5. Moreover, Figure 7b illustrates the confusion matrix attainable by the RHAR-EODELM approach on 30% of TSS. The figure

represented that the RHAR-EODELM approach has recognized 21, 21, 18, 21, 13, and 19 instances under classes 0-5. Similarly, Figure 7c exhibits the PR investigation of the RHAR-EODELM technique. The figures represented that the RHAR-EODELM method has gained extreme PR achievement under the total classes. Lastly, Figure 7d demonstrates the RHAR-EODELM model's ROC study. The figure illustrates that the RHAR-EODELM model has efficient outputs with utmost ROC values in diverse class labelling.

Table 4 and Figure 8 show HAR outcomes of the RHAR-EODELM approach with 70 and 30 percent of TRS/TSS under the USC HAD dataset. The outputs illustrate that the RHAR-EODELM approach has identified distinct classes. In the case with 70% of TRS, the RHAR-EODELM approach attains average $accu_y$ of 95.92%, $sens_y$ of 87.88%, $spec_y$ of 97.55%, F_{score} of 87.80%, and MCC of 85.43%. Similarly, with 30% of TSS, the RHAR-EODELM approach attains average $accu_y$ of 96.56%, $sens_y$ of 89.40%, $spec_y$ of 97.93%, F_{score} of 89.37%, and MCC of 87.76%.

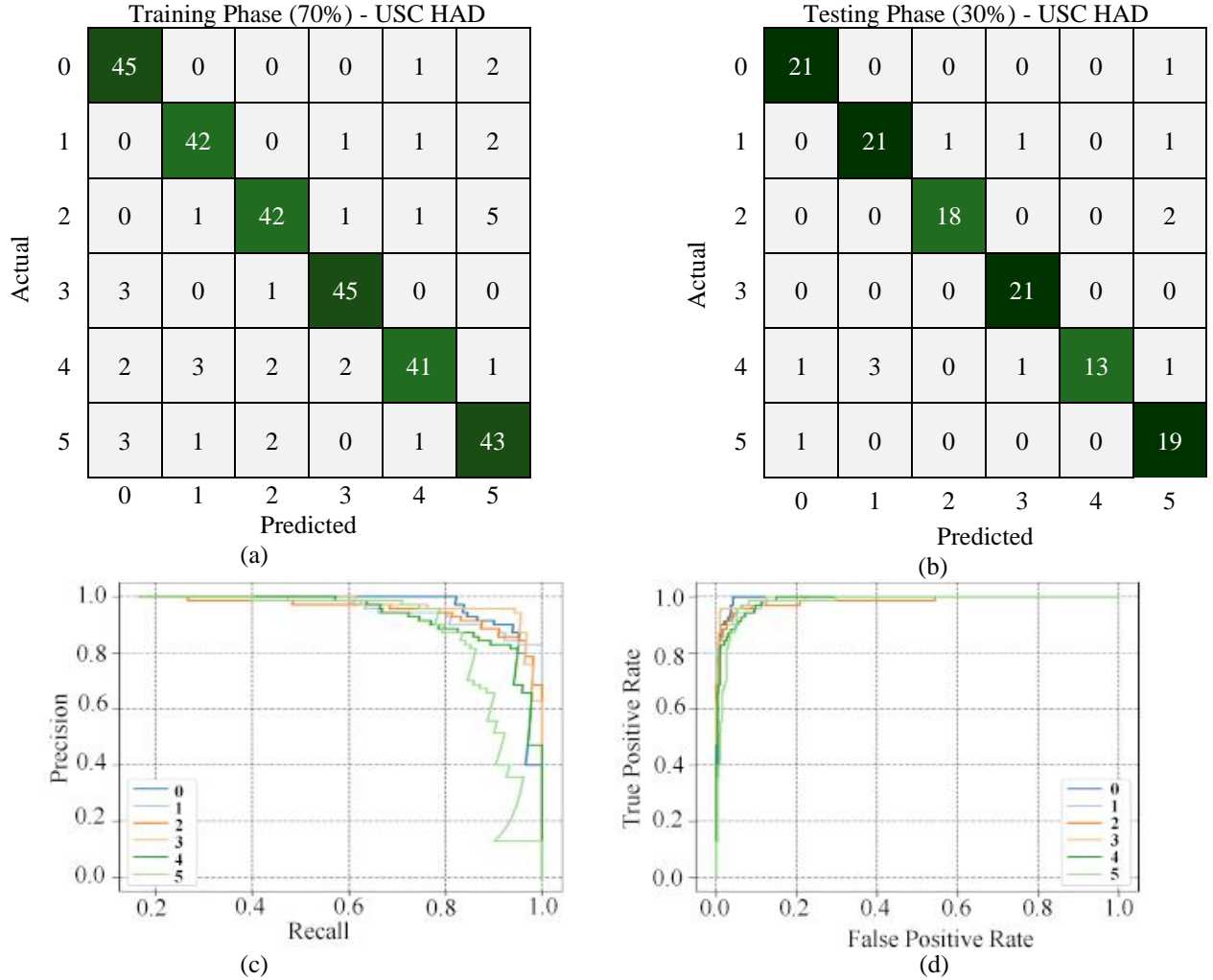


Fig. 7 Classifier outcome of USC HAD dataset (a-b) 70:30 of TRS/TSS, (c) PR, and (d) ROC

Table 4. HAR outcome of RHAR-EODELM technique with 70:30 of TRS/TSS on the USC HAD dataset

USC HAD					
Class	$Accu_y$	$Sens_y$	$Spec_y$	F_{score}	MCC
Training Phase (70%)					
0	96.26	93.75	96.75	89.11	87.01
1	96.94	91.30	97.98	90.32	88.51
2	95.58	84.00	97.95	86.60	84.01
3	97.28	91.84	98.37	91.84	90.20
4	95.24	80.39	98.35	85.42	82.82
5	94.22	86.00	95.90	83.50	80.04
Average	95.92	87.88	97.55	87.80	85.43
Testing Phase (30%)					
0	97.62	95.45	98.08	93.33	91.92
1	95.24	87.50	97.06	87.50	84.56
2	97.62	90.00	99.06	92.31	90.94
3	98.41	100.00	98.10	95.45	94.64
4	95.24	68.42	100.00	81.25	80.49
5	95.24	95.00	95.28	86.36	84.02
Average	96.56	89.40	97.93	89.37	87.76

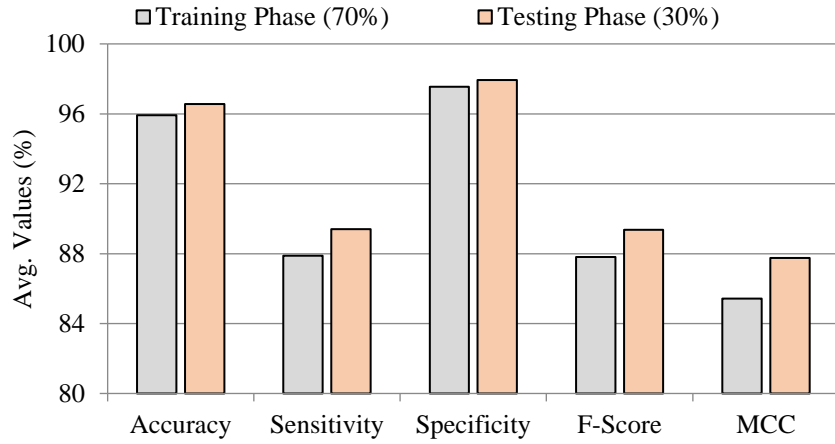


Fig. 8 Average outcome of RHAR-EODELM technique on the USC HAD dataset

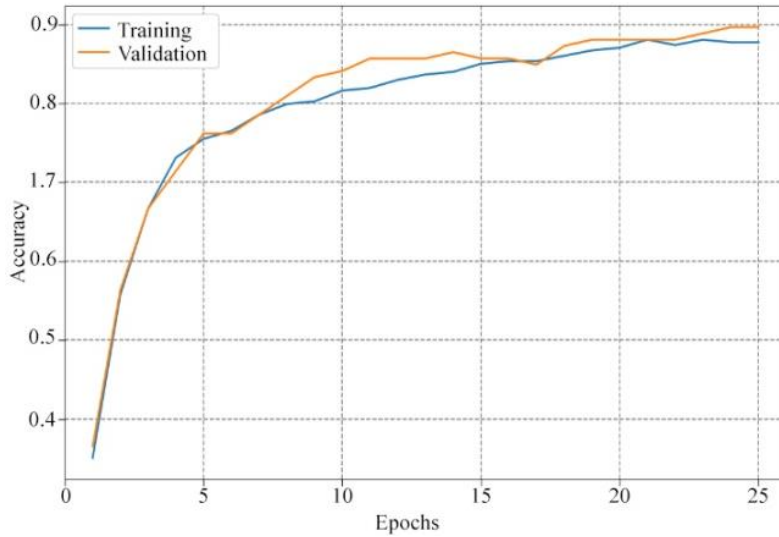


Fig. 9 TACC and VACC result of RHAR-EODELM technique on USC HAD dataset

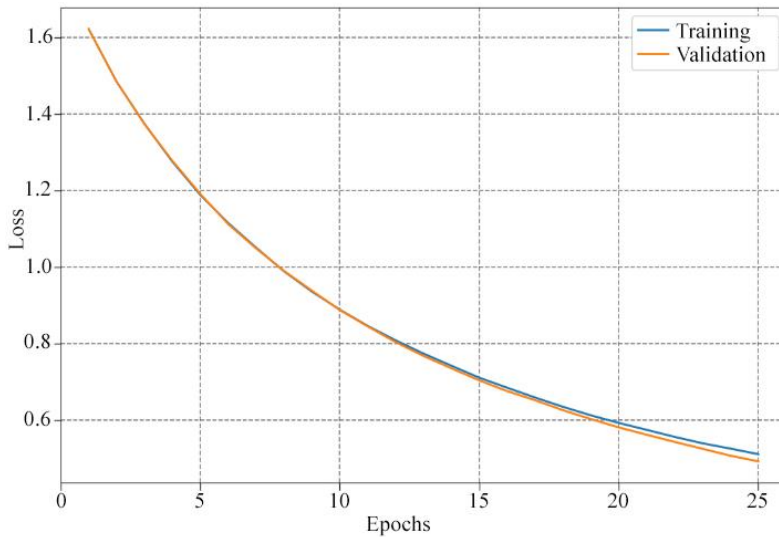


Fig. 10 TLS and VLS outcome of RHAR-EODELM approach on USC HAD dataset

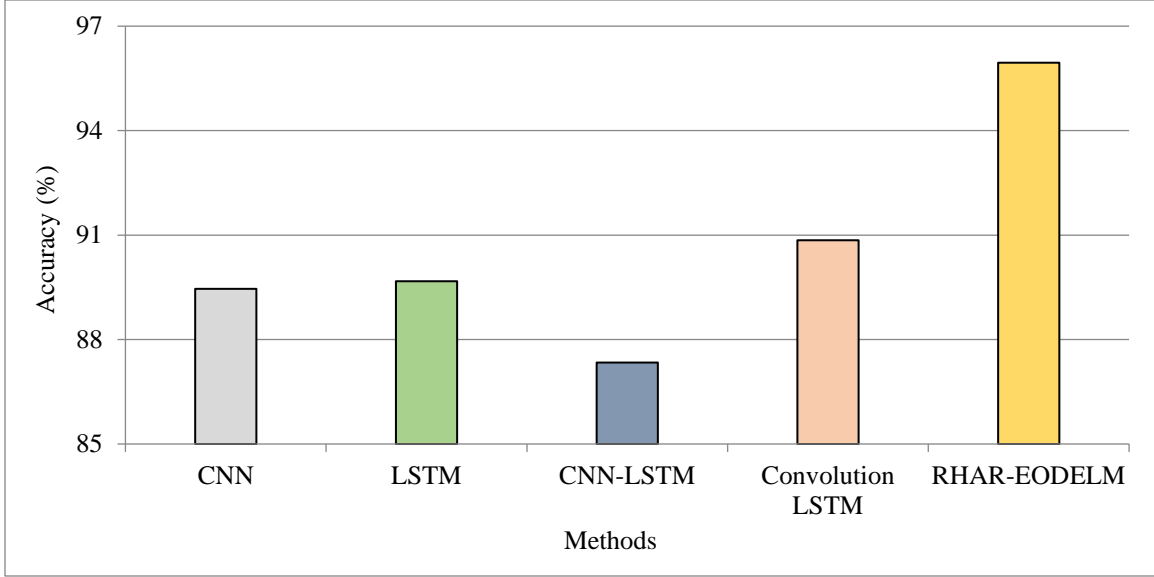


Fig. 11 Accu, analysis of the RHAR-EODELM approach under the UCI HAR dataset

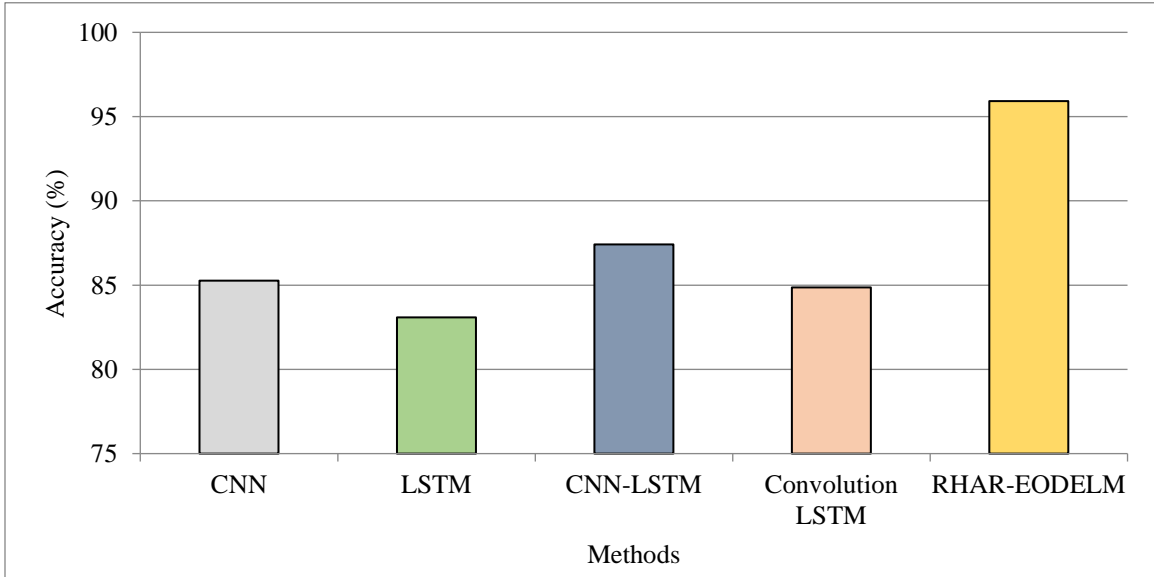


Fig. 12 Accu, analysis of the RHAR-EODELM approach under the USC HAD dataset

Table 5. Relative investigation of the RHAR-EODELM approach with other systems under two datasets

Methods	UCI HAR	USC HAD
CNN	89.456	85.264
LSTM	89.674	83.084
CNN-LSTM	87.339	87.414
Convolution LSTM	90.851	84.862
RHAR-EODELM	95.950	95.920

The TACC and VACC of the RHAR-EODELM model on the USC HAD database are represented in Figure 9. The figure denoted that the RHAR-EODELM model has enhanced achievement with enhanced TACC and VACC values. In particular, the RHAR-EODELM model has maximal TACC results. The TLS and VLS values of the

RHAR-EODELM technique on the USC HAD database are exemplified in Figure 10. The represented figure concluded that the RHAR-EODELM model has enhanced achievement with lesser TLS and VLS values. Seemingly the RHAR-EODELM technique has mitigated VLS outputs.

Table 5 provides a relative examination of the RHAR-EODELM technique with existing models [30]. Figure 11 depicts a relative training of the RHAR-EODELM technique with other DL models under the UCI HAR database. The figure demonstrates that the CNN-LSTM technique reaches the least $accu_y$ of 87.339%. Next, the CNN and LSTM models attain closer $accu_y$ of 89.456% and 89.674%, respectively. Meanwhile, the Conv. LSTM technique obtains reasonable $accu_y$ of 90.851%.

However, the RHAR-EODELM technique reaches a higher $accu_y$ of 95.950%. Figure 12 demonstrated a relative training of the RHAR-EODELM method with other DL approaches under the USC HAD dataset. The outputs demonstrate that the LSTM approach attains a minimum $accu_y$ of 83.084%. Next, the CNN and Conv. LSTM methods attain closer $accu_y$ of 85.264% and 84.862%, correspondingly. In the meantime, the CNN method gets a reasonable $accu_y$ of 85.264%. But, the RHAR-EODELM technique reaches a higher $accu_y$ of 95.920%. These results

exhibited the maximum performance of the RHAR-EODELM technique.

5. Conclusion

In this research, an automated activity recognition method termed the RHAR-EODELM model, is developed. The presented RHAR-EODELM technique mainly identified different classes of human activities. It follows a three-stage process. Initially, the RHAR-EODELM technique employs a min-max normalization process for scaling the activity data. Next, the RHAR-EODELM technique exploited the DELM-RBF model for the prediction process. Lastly, the EO model is implemented for adjusting the parameters relevant to the DELM-RBF method. To highlight the enriched HAR outcomes of the RHAR-EODELM method, a large scale of simulations was achieved. The simulation values signify that the RHAR-EODELM approach reaches improved predictive outcomes over other models. Later, the efficiency of the RHAR-EODELM technique will be boosted by hybrid DL methods.

References

- [1] Shibo Zhang et al., "Deep Learning in Human Activity Recognition with Wearable Sensors: A Review on Advances," *Sensors*, vol. 20, no. 4, pp. 1-43, 2022. [[CrossRef](#)] [[Google Scholar](#)] [[Publisher Link](#)]
- [2] Bolu Oluwalade et al., "Human Activity Recognition using Deep Learning Models on Smartphones and Smart Watches Sensor Data," *In Proceedings of 14th International Joint Conference on Biomedical Engineering Systems and Technologies*, pp. 1-6, 2021. [[CrossRef](#)] [[Google Scholar](#)] [[Publisher Link](#)]
- [3] Vittorio Mazzia et al., "Action Transformer: A Self-Attention Model for Short-Time Pose-Based Human Action Recognition," *Pattern Recognition*, vol. 124, pp.108487, 2022. [[CrossRef](#)] [[Google Scholar](#)] [[Publisher Link](#)]
- [4] Fuqiang Gu et al., "A Survey on Deep Learning for Human Activity Recognition," *ACM Computing Surveys (CSUR)*, vol. 54, no. 8, pp. 1-34, 2021. [[Google Scholar](#)] [[Publisher Link](#)]
- [5] K. Karthiga, and P. Karpagavalli, "An Efficient Human Tracking System using Local Binary Pattern and Cellular Non-Linear Networks," *International Journal of P2P Network Trends and Technology*, vol. 10, no. 5, pp. 1-6, 2020. [[CrossRef](#)] [[Publisher Link](#)]
- [6] Sakorn Mekruksavanich, and Anuchit Jitpattanakul, "Multimodal Wearable Sensing for Sport-Related Activity Recognition using Deep Learning Networks," *Journal of Advances in Information Technology*, vol. 13, no. 2, pp. 132-138, 2022. [[CrossRef](#)] [[Google Scholar](#)] [[Publisher Link](#)]
- [7] Wan Shaohua et al., "Deep Learning Models for Real-Time Human Activity Recognition with Smartphones," *Mobile Networks and Applications*, vol. 25, no. 2, pp. 743-755, 2020. [[CrossRef](#)] [[Google Scholar](#)] [[Publisher Link](#)]
- [8] Rajit Nair et al., "Impact of Wireless Sensor Data Mining with Hybrid Deep Learning for Human Activity Recognition," *Wireless Communications and Mobile Computing*, vol. 2022, pp. 1-8, 2022. [[CrossRef](#)] [[Google Scholar](#)] [[Publisher Link](#)]
- [9] S. Aswath, and S. Valarmathi, "Obstructive Sleep Apnea Severity Prediction Model GUI using Anthropometrics," *SSRG International Journal of Electrical and Electronics Engineering*, vol. 9, no. 12, pp. 134-144, 2022. [[CrossRef](#)] [[Publisher Link](#)]
- [10] J. A. Smitha et al., "Optimized Routing on Wireless Body Sensor Network using Adaptive Lion Optimization Algorithm for IoT," *SSRG International Journal of Electrical and Electronics Engineering*, vol. 9, no. 12, pp. 189-197, 2022. [[CrossRef](#)] [[Google Scholar](#)] [[Publisher Link](#)]
- [11] Pooja G Nair, and R. Sneha, "A Review: Facial Recognition using Machine Learning," *International Journal of Recent Engineering Science*, vol. 7, no. 3, pp. 85-89, 2020. [[CrossRef](#)] [[Publisher Link](#)]
- [12] Linkai Li et al., "Integrated Access Control System of Face Recognition and Non-Contact Temperature Measurement Based on Arduino," *International Journal of Computer and Organization Trends*, vol. 12, no. 2, pp. 1-5, 2022. [[CrossRef](#)] [[Publisher Link](#)]
- [13] C. Nithyeswari, and G. Karthikeyan, "An Ensemble of Deep Learning with Optimization Model for Activity Recognition in the Internet of Things Environment," *SSRG International Journal of Electrical and Electronics Engineering*, vol. 10, no. 4, pp. 91-104, 2023. [[CrossRef](#)] [[Publisher Link](#)]

- [14] Yujie Wang, Lu Yao, Ying Wang, and Yong Zhang, "Robust CSI-based Human Activity Recognition with Augmented Few-Shot Learning," *IEEE Sensors Journal*, vol. 21, no. 21, pp. 24297-24308. [[CrossRef](#)] [[Google Scholar](#)] [[Publisher Link](#)]
- [15] Chaobo Li, Xulin Shen, and Hongjun Li, "S3GRN: Structural Similar Stepwise Generative Recognizable Network for Human Action Recognition with Limited Training Data," *IEEE Access*, vol. 8, pp. 216219-216230, 2020. [[CrossRef](#)] [[Google Scholar](#)] [[Publisher Link](#)]
- [16] Goutham Sakthivinayagam et al., "Violence Detection System using Convolution Neural Network," *SSRG International Journal of Electronics and Communication Engineering*, vol. 6, no. 2, pp. 5-8, 2019. [[CrossRef](#)] [[Google Scholar](#)] [[Publisher Link](#)]
- [17] Santosh Kumar Yadav et al., "Skeleton-Based Human Activity Recognition using ConvLSTM and Guided Feature Learning," *Soft Computing*, vol. 26, no. 2, pp. 877-890, 2022. [[CrossRef](#)] [[Google Scholar](#)] [[Publisher Link](#)]
- [18] Muhammad Bilal et al., "A Transfer Learning-Based Efficient Spatiotemporal Human Action Recognition Framework for Long and Overlapping Action Classes," *The Journal of Supercomputing*, vol. 78, no. 2, pp. 2873-2908, 2022. [[CrossRef](#)] [[Google Scholar](#)] [[Publisher Link](#)]
- [19] Yong Li, and Luping Wang, "Human Activity Recognition Based on Residual Network and BiLSTM," *Sensors*, vol. 22, no. 2, pp. 635, 2022. [[CrossRef](#)] [[Google Scholar](#)] [[Publisher Link](#)]
- [20] Imran Ullah Khan, Sitara Afzal, and Jong Weon Lee, "Human Activity Recognition via Hybrid Deep Learning Based Model," *Sensors*, vol. 22, no. 1, pp. 323, 2022. [[CrossRef](#)] [[Google Scholar](#)] [[Publisher Link](#)]
- [21] Huaijun Wang et al., "Wearable Sensor-Based Human Activity Recognition using Hybrid Deep Learning Techniques," *Security and Communication Networks*, vol. 2020, pp. 1-12, 2020. [[CrossRef](#)] [[Google Scholar](#)] [[Publisher Link](#)]
- [22] Ohoud Nafea et al., "Sensor-Based Human Activity Recognition with Spatio-Temporal Deep Learning," *Sensors*, vol. 21, no. 6, pp. 2141, 2021. [[CrossRef](#)] [[Google Scholar](#)] [[Publisher Link](#)]
- [23] Mohamed Abdel-Basset et al., "ST-DeepHAR: Deep Learning Model for Human Activity Recognition in IoT Applications," *IEEE Internet of Things Journal*, vol. 8, no. 6, pp. 4969-4979, 2020. [[CrossRef](#)] [[Google Scholar](#)] [[Publisher Link](#)]
- [24] Kamal A. ElDahshan, AbdAllah A. AlHabshy, and Bashar I. Hameed, "Meta-Heuristic Optimization Algorithm-Based Hierarchical Intrusion Detection System," *Computers*, vol. 11, no. 12, pp. 170, 2022. [[CrossRef](#)] [[Google Scholar](#)] [[Publisher Link](#)]
- [25] Dezheng Zhang, Peng Li, and Aziguli Wulamu, "An Improved Multi-Label Learning Method with ELM-RBF and a Synergistic Adaptive Genetic Algorithm," *Algorithms*, vol. 15, no. 6, pp. 185, 2022. [[CrossRef](#)] [[Google Scholar](#)] [[Publisher Link](#)]
- [26] Janandra Krishna Kishore Dokala et al., "A New Meta-Heuristic Optimization Algorithm Based MPPT Control Technique for PV System Under Diverse Partial Shading Conditions," 2022. [[CrossRef](#)] [[Google Scholar](#)] [[Publisher Link](#)]
- [27] P. Dhivya Bharathy et al., "Hand Gesture Recognition for Physical Impairment Peoples," *SSRG International Journal of Computer Science and Engineering*, vol. 4, no. 10, pp. 6-10, 2017. [[CrossRef](#)] [[Publisher Link](#)]
- [28] [Online]. Available: <https://archive.ics.uci.edu/ml/datasets/human+activity+recognition+using+smartphones>
- [29] [Online]. Available: <http://sipi.usc.edu/had/>
- [30] Sakorn Mekruksavanich, and Anuchit Jitpattanakul, "Biometric User Identification based on Human Activity Recognition using Wearable Sensors: An Experiment using Deep Learning Models," *Electronics*, vol. 10, no. 3, pp. 308, 2021. [[CrossRef](#)] [[Google Scholar](#)] [[Publisher Link](#)]